

---

# FAIR Universe

## HiggsML Uncertainty Challenge Competition

---

Wahid Bhimji<sup>1</sup>, Paolo Calafiura<sup>1</sup>, Ragansu Chakkappai<sup>2,6</sup>, Po-Wen Chang<sup>1</sup>, Yuan-Tang Chou<sup>3</sup>,  
 Sascha Diefenbacher<sup>1</sup>, Jordan Dudley<sup>4,1</sup>, Steven Farrell<sup>1</sup>, Aishik Ghosh<sup>5,1</sup>, Isabelle Guyon<sup>6</sup>, Chris  
 Harris<sup>1</sup>, Shih-Chieh Hsu<sup>3</sup>, Elham E Khoda<sup>7,3,1</sup>, Rémy Lyscar<sup>2</sup>, Alexandre Michon<sup>2</sup>, Benjamin  
 Nachman<sup>1</sup>, Peter Nugent<sup>1</sup>, Mathis Reymond<sup>8</sup>, David Rousseau<sup>2,6</sup>, Benjamin Sluijter<sup>9,1</sup>, Benjamin  
 Thorne<sup>1</sup>, Ihsan Ullah<sup>6</sup>, and Yulei Zhang<sup>3</sup>

<sup>1</sup>Lawrence Berkeley National Laboratory  
<sup>2</sup>Université Paris-Saclay, CNRS/IN2P3, IJCLab  
<sup>3</sup>University of Washington, Seattle  
<sup>4</sup>University of California, Berkeley  
<sup>5</sup>University of California, Irvine  
<sup>6</sup>ChaLearn  
<sup>7</sup>University of California, San Diego  
<sup>8</sup>Université Paris-Saclay  
<sup>9</sup>Universiteit Leiden

[fair-universe@lbl.gov](mailto:fair-universe@lbl.gov)  
<https://fair-universe.lbl.gov>

Compiled: December 19, 2024

### Abstract

The FAIR Universe – HiggsML Uncertainty Challenge focuses on measuring the physics properties of elementary particles with imperfect simulators due to differences in modelling systematic errors. Additionally, the challenge is leveraging a large-compute-scale AI platform for sharing datasets, training models, and hosting machine learning competitions. Our challenge brings together the physics and machine learning communities to advance our understanding and methodologies in handling systematic (epistemic) uncertainties within AI techniques.

## Contents

<b>1</b>	<b>Introduction</b>	<b>3</b>
1.1	Background and impact . . . . .	3
1.2	Novelty . . . . .	3
<b>2</b>	<b>Data</b>	<b>4</b>
<b>3</b>	<b>Tasks and application scenarios</b>	<b>5</b>
<b>4</b>	<b>Metrics</b>	<b>5</b>
<b>5</b>	<b>Baselines, code, and material provided</b>	<b>7</b>
5.1	Website, tutorial and documentation . . . . .	9
<b>6</b>	<b>Organizational aspects</b>	<b>9</b>
6.1	Overview . . . . .	9
6.2	Competition Protocol . . . . .	10
<b>7</b>	<b>Conclusions and Outlook</b>	<b>12</b>
<b>A</b>	<b>Proton collisions and detection</b>	<b>17</b>
<b>B</b>	<b>Special relativity</b>	<b>19</b>
B.1	Momentum, mass, and energy . . . . .	19
B.2	Invariant mass . . . . .	19
B.3	Other useful formulas . . . . .	20
<b>C</b>	<b>The detailed description of the features</b>	<b>21</b>
<b>D</b>	<b>Systematic biases</b>	<b>24</b>
D.1	Systematic bias definition . . . . .	24
D.2	Impact of biases on features . . . . .	24
D.3	Weight impacting bias implementation . . . . .	25
D.4	Event selection . . . . .	25

# 1 Introduction

## 1.1 Background and impact

For several decades, the discovery space in almost all branches of science has been accelerated dramatically due to increased data collection brought on by the development of larger, faster instruments. More recently, progress has been further accelerated by the emergence of powerful AI approaches, including deep learning, to exploit these data. However, an unsolved challenge that remains, and *must* be tackled for future discovery, is how to effectively quantify and reduce uncertainties, including understanding and controlling *systematic* uncertainties (also named *epistemic* uncertainties in other fields). This is widely true across scientific and industrial applications involving measurement instruments (medicine, biology, climate science, chemistry, and physics, to name a few). A compelling example is found in analyses to further our fundamental understanding of the universe through analysis of the vast volumes of particle physics data produced at CERN, in the **Large Hadron Collider (LHC)**.

Ten years ago, part of our team co-organised the **Higgs Boson Machine Learning Challenge** (HiggsML) [1], the most popular Kaggle challenge at the time attracting 1785 teams. This challenge has significantly heightened interest in applying Machine Learning (ML) techniques within High-Energy Physics and, conversely, has exposed physics issues to the ML community. Whereas previously, the most effective methods predominantly relied on boosted decision trees, Deep Learning has since gained prominence (see, e.g., **HEP ML living review**). While the LHC has not (yet) discovered new physics beyond the Higgs boson, it has accumulated vast data and will continue to accumulate more data well into the next decade. There is a discovery potential in very precise measurements of particle properties, in particular the Higgs boson which can only be studied at the LHC. This demands meticulous measurement of uncertainties and their incorporation into developing sophisticated AI techniques.

High energy physics (HEP) relies on statistical analysis of aggregated observations. Therefore, the interest in uncertainty-aware ML methods in HEP is nearly as old as the application of ML in the field. Advanced efforts that integrate uncertainties into the ML training include approaches that explicitly depend on nuisance parameters [2–9], that are insensitive to nuisance parameters [10–27], that use downstream test statistics in the initial training [28–36], and that use Bayesian neural networks for estimating uncertainties [37–40]. Many of these topics were covered in a forward-looking review-type article in Ref. [41]. However, these developments all report technique performance on different ad-hoc datasets, so it is difficult to compare their merits. This competition aims at providing a common ground, with a dataset of sufficient complexity, equipped with systematic bias parameterisations, and a metric.

We aim to address the issue of systematic uncertainties within a specific domain. Yet, the techniques developed by the challenge participants will apply to identifying, quantifying, and correcting systematic uncertainties in other areas. A critical aspect of this work is to provide a dataset and platform that conforms to the principles of findability, accessibility, interoperability, and reusability - inspiring the name of our project: FAIR Universe. We plan to keep our submission platform accessible even after the challenge concludes, establishing it as a lasting benchmark. This initiative should significantly influence research in uncertainty-aware AI/ML techniques, which currently suffer from a critical shortage of datasets and benchmarks dedicated to their research and development.

## 1.2 Novelty

This entirely new public competition builds on our experience running several competitions in particle physics and broader. These include the original HiggsML data challenge [1], the TrackML Challenges (NeurIPS 2018 competition) [42, 43], the LHC Olympics [44], AutoML/AutoDL [45, 46], and other competitions. Building on the foundation of the original HiggsML challenge, this competition introduces a significant change by using simulated data that includes biases (or *systematic effects*) in the test dataset. In addition, participants are asked to provide a confidence interval and not just a point estimate. We have developed an innovative metric to assess their performance.

While there have been previous challenges focusing on meta-learning and transfer-learning, such as the **NeurIPS 2021 and 2022 meta-learning challenges** [47, 48], **Unsupervised and Transfer Learning** [49], challenges related to bias e.g. **Crowd bias challenge** [50], and those addressing distribution shifts,

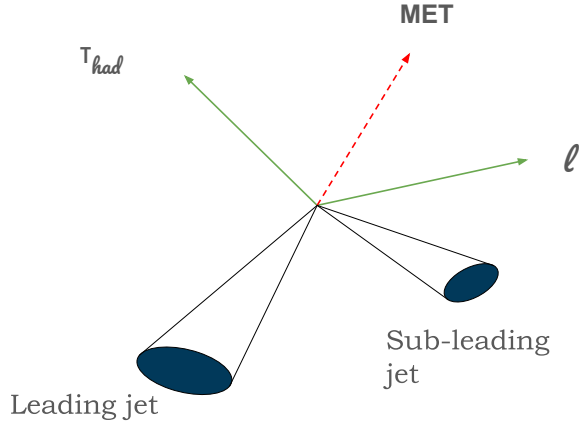


Figure 1: Diagram of the particles in the final state chosen: one lepton, one tau hadron, up to two jets, and the missing transverse momentum vector, see [Appendix A](#) for details.

like the [Shifts challenge series](#), and [CCAI@UNICT 2023](#) [51], to the best of our knowledge, this is the first challenge that requires participants to handle systematic uncertainty.

Moreover, this project is connecting the [Perlmutter system at NERSC](#), a large-scale supercomputing resource featuring over 7000 NVIDIA A100 GPUs, with [Codabench](#), a new version of the [renowned open-source benchmark platform Codalab competitions](#). Our challenge is among the first to utilise this platform for a public competition, marking a significant milestone in accessible, high-performance computing for AI research.

## 2 Data

We are using a simulated particle physics dataset for this competition to produce data representative of high energy proton collision data collected by the ATLAS experiment [52] at the Large Hadron Collider (LHC) [53]. The dataset is created using two widely used simulation tools, Pythia 8.2 [54] and Delphes 3.5.0 [55]. We have organised the dataset into a tabular format where each row corresponds to a collision event with 28 features, the measurements recorded from a single proton bunch crossing of interest (see [Appendix A](#)). The detailed list of features is available in [Appendix C](#), preceded by a brief introduction to special relativity that can be used to understand them better [Appendix B](#). The events are divided into two categories (see [Table 1](#)): signal and background. The signal category includes collision events with a Higgs boson decaying into tau pairs (see [Figure 1](#)) (one decaying into a lepton, the other one into a hadronic tau), while the background category includes other processes (subcategories) leading to a similar final state.

Due to its complexity, the process of generating events is computationally intensive; use of the Perlmutter supercomputer allowed us to create a vast amount of data, about 280 million events, which is almost three orders of magnitude larger than for the HiggsML competition. It will be made publicly available under the Creative Commons Attribution license to serve as a benchmark dataset after the competition.

In addition, we have developed a biasing script capable of manipulating a dataset by introducing six parameterised distortions as a function of six *Nuisance Parameters*<sup>1</sup> (the systematic biases); see details in [Appendix D](#). For example, a detector miscalibration can cause a bias in other features in a cascade way, or in another case, the magnitude of a particular background (e.g. the  $t\bar{t}$ ) contribution

<sup>1</sup>The name Nuisance Parameter, commonly used in the physics literature, refers to a parameter governing a specific parameterisation of a systematic bias. Nuisance Parameters can be in part constrained from the data itself but the name implies that constraining them is only interesting as an auxiliary task in the process of determining a parameter of interest like the signal strength  $\mu$ .

Table 1: Summary of the dataset for each category and subcategory. "Number Generated" is the number of events available. In contrast, "LHC events" is the average number in this category in a pseudo-experiment corresponding to running of the Large Hadron Collider for  $10 \text{ fb}^{-1}$ , corresponding to approximately 800 billion inelastic proton collisions, or 2 weeks in summer 2024 conditions.

Process	Number Generated	LHC Events	Label
Higgs	52101127	1015	<b>signal</b>
Z Boson	221724480	1002395	<b>background</b>
Di-Boson	2105415	3783	<b>background</b>
$t\bar{t}$	12073068	44190	<b>background</b>

can change so that the composition of the background (thus the feature distributions) can be different. In both cases, the inference would be done on a dataset not i.i.d to the training dataset.

To avoid any leakage, the dataset, with all labels, was handled on the private disks of just two team members before being uploaded to Codabench, where it is secured. The random generator seeds, which could be used to reproduce the dataset, are also secured.

### 3 Tasks and application scenarios

The participant’s objective is to develop an estimator for the number of Higgs boson events in a dataset analogous to results from Large Hadron Collider experiments. Such a measurement is typical to those carried over at the Large Hadron Collider, which allows us to strengthen (or invalidate!) our understanding of the fundamental laws of nature.

The primary metric is the *signal strength* ( $\mu$ ), which is the number of estimated Higgs boson events divided by the number of such events predicted by the Standard Model, which is the reference theory. The challenge involves estimating  $\mu$ ’s true value,  $\mu_{true}$ , which may vary from one (in practice in the range 0.1 to 3) and is inherently unknown.

Participants are tasked with generating a 68.27% Confidence Interval (CI) for  $\mu$ , incorporating both aleatoric (random) and epistemic (systematic) uncertainties rather than a single-point estimate. The implementation of the six different systematic uncertainties is detailed in [Appendix D](#).

The primary simulation dataset assumes a  $\mu$  of one. Participants receive a training subset, where events are labelled based on their event type (e.g. Higgs boson event). The organisers provide the script to generate unlabelled pseudo-experiment datasets from the primary simulation dataset for any value of  $\mu$  and the six systematic biases. The participant’s model should be able to reverse the process and provide a 68.27% CI on  $\mu$  for any pseudo-experiment.

In a machine learning context, the task resembles a transduction problem with distribution shift: it requires constructing a  $\mu$  interval estimator from labelled training data and biased unlabelled test data. One possibility is to train a classifier to distinguish Higgs boson from the background, with robustness against bias achieved possibly through data augmentation (or an adversarial approach, or black box optimization or any other novel approach) via the provided script.

This challenge shifts focus from the qualitative discovery of individual Higgs boson events (which was the focus of our first challenge) to the quantitative estimation of overall Higgs boson counts in test sets, akin to assessing disease impact on populations rather than diagnosing individual cases.

### 4 Metrics

Participants must submit a model to the Codabench platform that can analyse a dataset to determine  $(\mu_{16}, \mu_{84})$ , which represents the bounds of the 68.27% Confidence Interval (CI) for  $\mu$ .

The model’s performance is assessed based on two criteria:

- **Precision:** The narrowness of the CI (narrower is preferable).

- **Coverage:** The accuracy of the CI in reflecting the measurement’s uncertainty, meaning there should be a 68.27% probability that  $\mu_{\text{truth}}$  falls within the CI.

The model that predicts  $(\mu_{16}, \mu_{84})$  serves as an estimator. In statistics, the effectiveness of an estimator is not evaluated based on a single case but rather over numerous instances. Therefore, the model undergoes evaluation across a series of  $N_{\text{test}}$  pseudo-experiments, each characterized by randomized biases and  $\mu_{\text{truth}}$ , to assess it against the specified criteria. We introduce a novel uncertainty metric, which we call **Coverage Score**. This metric is divided into two components:

The first component is the **Average Interval Width**  $w$ , calculated as follows:

$$w = \frac{1}{N_{\text{test}}} \sum_{i=1}^N |\mu_{84,i} - \mu_{16,i}|, \quad (1)$$

where  $\mu_{16,i}$  and  $\mu_{84,i}$  are the bounds of the 68.27% CI for each experiment  $i$  within the range  $[1, N_{\text{test}}]$ .

The second component  $c$  quantifies the frequency with which the true value of  $\mu_{\text{true}}$  falls within the 68.27% Confidence Interval (CI), as illustrated in Figure 2:

$$c = \frac{1}{N_{\text{test}}} \sum_{i=1}^N 1 \text{ if } \mu_{\text{true},i} \in [\mu_{16,i} - \mu_{84,i}]. \quad (2)$$

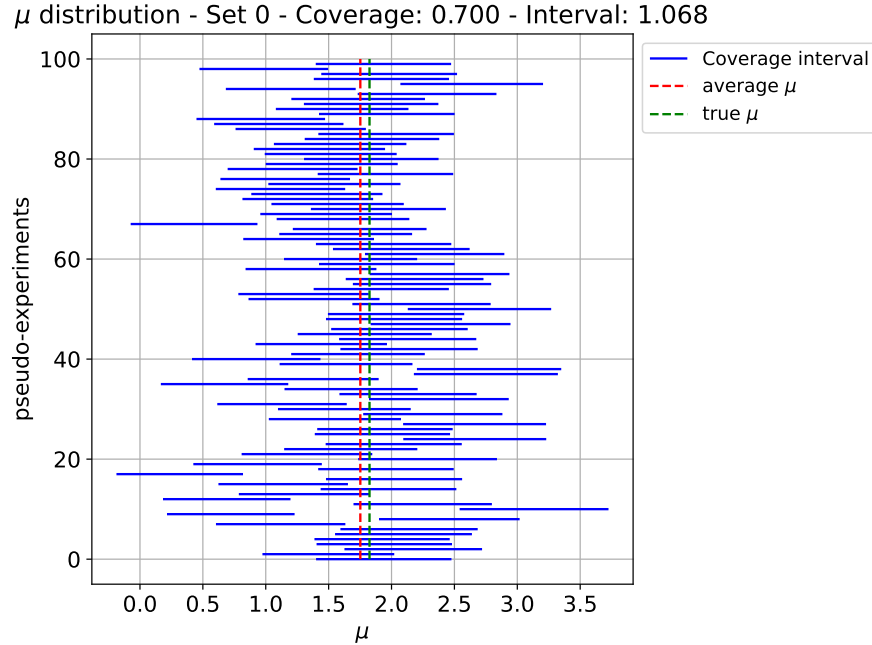


Figure 2: *Coverage plot:* all the predicted intervals (blue lines) for each pseudo experiment generated for a given  $\mu_{\text{true}}$  (vertical dotted line). The coverage (here  $70 \pm 5\%$ ) is determined by the fraction of time the horizontal blue lines intersect the vertical line. The average width of the interval is here 1.068.

If the confidence interval  $[\mu_{16,i}, \mu_{84,i}]$  accurately represents the 68.27% quantile, the true value of  $\mu$  should lie within this interval in 68.27% of the pseudo-experiments. Consequently, we employ a penalising function  $f$  that penalises models that deviate from this 68.27% reference (Figure 3) :

$$c \in [0.6827 - 2\sigma_{68}, 0.6827 + 2\sigma_{68}] : f(c) = 1 \quad (3)$$

$$c < 0.6827 - 2\sigma_{68} : f(c) = 1 + \left| \frac{c - (0.6827 - 2\sigma_{68})}{\sigma_{68}} \right|^4 \quad (4)$$

$$c > 0.6827 + 2\sigma_{68} : f(c) = 1 + \left| \frac{c - (0.6827 + 2\sigma_{68})}{\sigma_{68}} \right|^3 \quad (5)$$

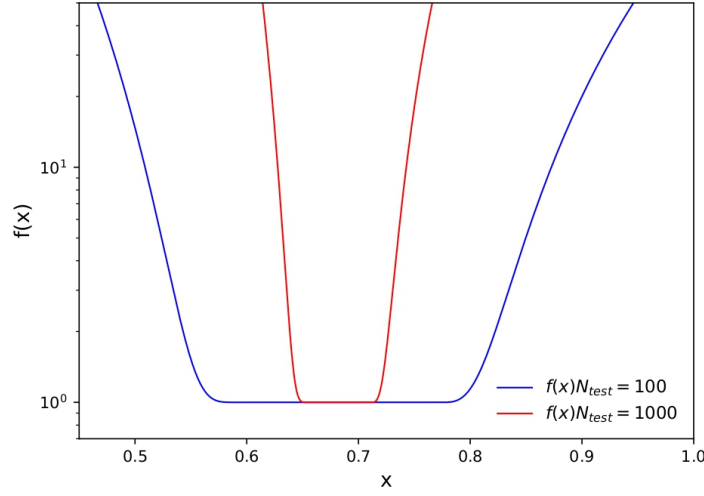


Figure 3: Penalising function as a function of the coverage value  $c$ . The shape of the function is determined by uncertainty on the coverage evaluation, governed by  $N_{test}$ , the number of pseudo-experiments. A larger  $N_{test}$  leads to a narrower function.

Here,  $\sigma_{68}$  is the standard deviation for a binomial distribution with  $p = 0.6827$ , given by

$$\sigma_{68} = \sqrt{\frac{(1 - 0.6827)0.6827}{N_{test}}}, \quad (6)$$

this parameter establishes a tolerance zone around the anticipated value of 0.6827, accommodating statistical variances inherent in the evaluation process. We opted for an asymmetric penalty function because, within the field of High Energy Physics (HEP), overestimating uncertainty is deemed more acceptable than underestimating it [56, 57]. Hence, coverage exceeding 68.27% incurs a lesser penalty than coverage falling below 68.27%.

The final **Coverage Score** used to rank participants is calculated as follows:

$$\text{score} = -\ln((w + \epsilon)f(c)), \quad (7)$$

$w$  represents the average width of the Confidence Interval,  $c$  is the coverage parameter, and  $\epsilon = 10^{-2}$  is a regularization term to guard against submissions that report unrealistically narrow CIs. Using the  $-\ln()$  function ensures that higher scores are awarded to superior submissions and that the score variations remain within a modest range.

To ensure efficient use of resources and timely updates to the leaderboard, each participant's model inference is executed across 100 pseudo-experiments times five distinct values of  $\mu_{truth}$ . In the Final phase of the competition, the best submission from each participant will be evaluated over 1,000 pseudo-experiments, times ten different  $\mu_{truth}$  values, to minimize random noise in the evaluation.

## 5 Baselines, code, and material provided

A **Starting Kit** is available on the challenge website. This kit includes code for installing necessary packages, loading and visualising data, training and evaluating a model and preparing a submission

for the competition. This should facilitate local testing and adjustments by participants before their official submissions and allow them to train and evaluate models. Moreover, the competition adheres to a specific interface, details of which are documented in the Starting Kit and demonstrated through the provided sample code.

The Baseline method estimates  $\mu$  by using standard techniques without addressing systematic uncertainties directly for simplicity. Initially, it utilizes a classifier (based on XGBoost Boosted Decision Tree, or a simple PyTorch dense Neural Network) trained on BaselineTrain, a subset of training data to enhance signal event density and reduce  $\mu$  estimator variance. Although adjustable for variance optimization, the classifier's decision threshold is fixed heuristically.  $\mu$  is then estimated from these filtered events, assuming Poisson distribution, enabling point-wise and interval maximum likelihood estimation. Further refinement involves binning particles as per classifier score and estimating  $\mu$  per bin, akin to a voting ensemble. BaselineHoldout, a reserved training dataset, is used to predict the amount of background and signal in each bin for  $\mu=1$ . This calibration step then permits estimating  $\mu$  (and the corresponding Confidence Interval) on pseudo-experiment for  $\mu$  estimation. On Figure 4, the alignment of maximum likelihood estimation (orange line) with unlabelled data (black line) indicates method success, in the absence of any bias.

Now, when unknown biases occur, the prediction on the amount of background and signal event per bin will be wrong, biasing the estimation of  $\mu$ . To address the problem of systematic errors, participants are encouraged to enhance the Baseline model, for instance, by modifying the architecture or training protocol to improve resilience against biases, attempting to directly model the biases, or refining the estimator through a bias-aware model. Another way to see it is that, armed with the biasing script which can produce a dataset for any value of the six Nuisance Parameters and the signal strength  $\mu$ , the participants could train a model which could regress the seven parameters for any pseudo-experiment and report the Confidence Interval on  $\mu$ .

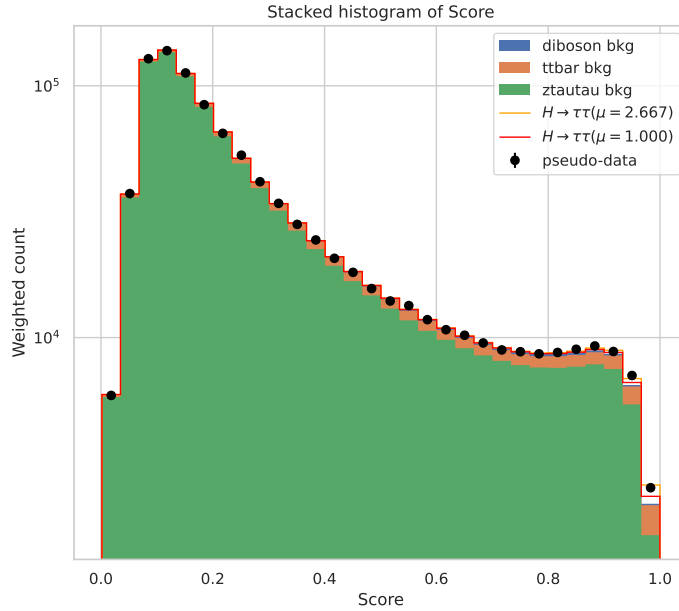


Figure 4: *Model Output*: Unlabelled test pseudo-data (black points), and HoldOut data for (1) background events  $Z \rightarrow \tau\tau$  (solid green), (2) background  $t\bar{t}$  (solid orange) (3) background di-boson (solid blue, hardly visible) (4) signal events  $H \rightarrow \tau\tau$  for  $\mu = 1$  (red line), and (5) signal events fitted histogram to test pseudo-data, leading to estimated  $\mu = 2.667$  (orange line).



## 5.1 Website, tutorial and documentation

We have set up a dedicated GitHub repository<sup>2</sup> for this competition and the competition’s Codabench website<sup>3</sup>. The GitHub repository covers the following points:

- Competition introduction and instructions for setting up the complete environment.
- Complete details of the evaluation process.
- Information about how to submit.
- Troubleshooting instructions for possible issues and contact details for reporting issues.
- Link to a dedicated forum on the Codabench platform for efficient communication.

In addition, a code tutorial is provided for: (i) loading and discovering properties of data. (ii) explaining the coding structure and expected functions to be implemented in submissions. (iii) providing instructions and examples for running the baseline methods on the public datasets.

## 6 Organizational aspects

### 6.1 Overview

#### Competition

The competition is hosted on **Codabench** platform with a dedicated webpage on Codabench. Participants are required to create accounts on the platform and register for the competition, accepting the competition’s rules, as listed on the site. Participants can see and access all the public details without registering for the competition. Both signing up to Codabench and registering for the competition have no fee.

#### Competition Phases

The competition consists of two phases:

- **Phase 1: Public Phase** – Participants submit their model
- **Phase 2: Final Phase** – Participants now submit only one best submission from the previous phase for final evaluation (by default, it would be one with the highest score).

#### Competition Pages

Participants are provided with multiple pages detailing the competition overview, evaluation procedures, data description, competition terms, starting kit, and public data.

#### Starting Kit

The starting kit is a tutorial notebook designed to familiarise participants with the competition protocol, competition data, scoring, and code to prepare their submissions for the competition website. Participants are also given some ready-to-submit submissions in the GitHub repository to get them started with libraries such as PyTorch [58], TensorFlow [59], scikit-learn [60] etc.

#### Submissions

Once registered, participants can submit their solutions (code submissions, possibly including training), which are executed on resources at the National Energy Research Scientific Computing Center (NERSC). Participants receive submission feedback once per day, as displayed on the competition leaderboard. Every submission is executed in the same environment with the same maximum execution time of 2 hours (for the complete evaluation), translating into about 10 second GPU maximum inference time for one pseudo-experiment. Each participant is allowed to make only five submissions per day and a maximum of 100 submissions during the challenge. To enable the participants to perform other experiments on their hardware, they can use the public data provided in Phase 1.

<sup>2</sup><https://github.com/FAIR-Universe/HEP-Challenge>

<sup>3</sup><https://www.codabench.org/competitions/2977/>

## Codabench Tutorial

We have prepared a codabench tutorial for participants to get started with the competition quickly. The tutorial gives all the steps to access the competition, public data, starting kit, dummy submission, and leaderboard. Furthermore, we have detailed the competition flow, submission process, and contact information at the end of the tutorial.

Tutorial link:

[https://fair-universe.lbl.gov/tutorials/Higgs\\_Uncertainty\\_Challenge-Codabench\\_Tutorial.pdf](https://fair-universe.lbl.gov/tutorials/Higgs_Uncertainty_Challenge-Codabench_Tutorial.pdf)

## 6.2 Competition Protocol

Participants can either submit a pre-trained model or train their model as part of the submission. When a participant uploads the submission to the competition, that code is executed by the following two steps (summarized in Figure 5 and Figure 6).

### Ingestion

The ingestion step executes an ingestion program that is responsible for the following:

- loads train data
- loads test data (without labels)
- initializes the submitted model
- calls the fit method of the submitted model (to be used for training a model or loading a pre-trained model that is submitted together with the submission)
- calls the predict method multiple times (once for each test set) to get predictions (mu\_hat, delta\_mu\_hat, p16, and p84)
- saves the predictions for the scoring program

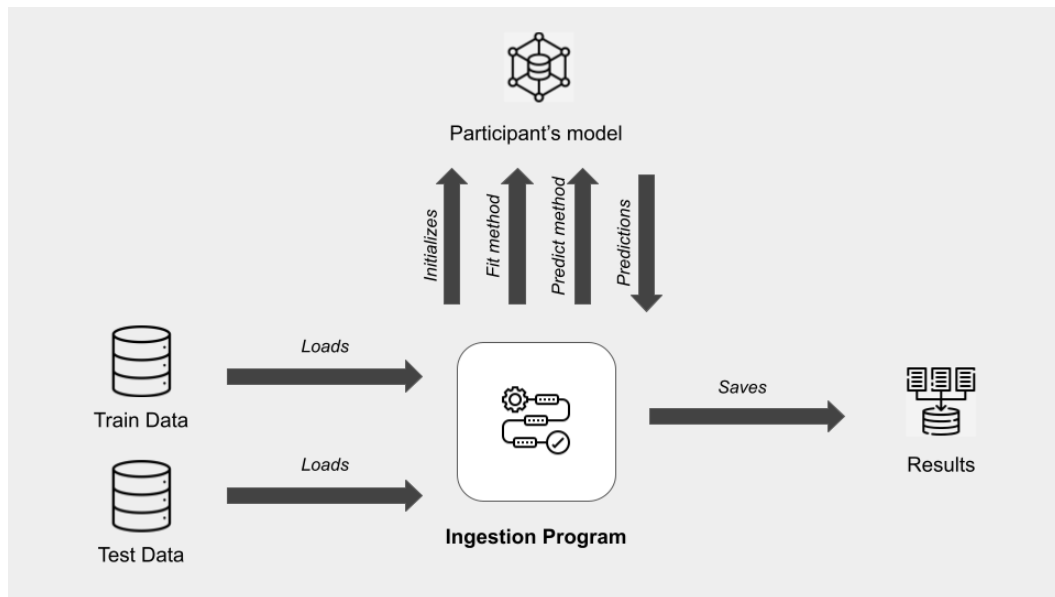


Figure 5: Ingestion Program execution flow

### Scoring

The scoring step executes a scoring program that is responsible for the following:

- loads the predictions saved by the ingestion program

- loads the ground truth or test settings
- calculates scores
- saves scores and detailed results

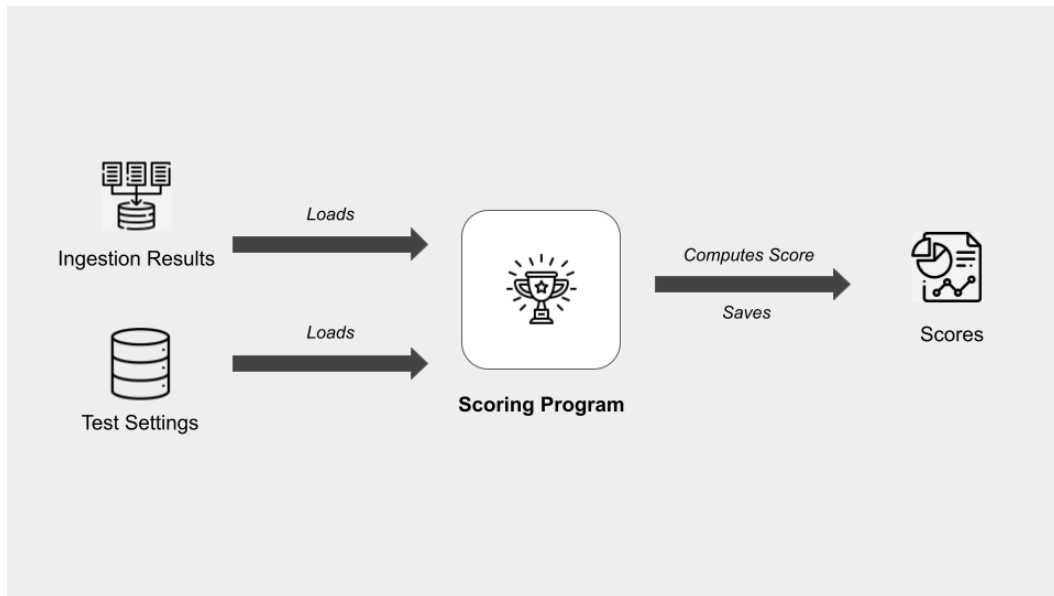


Figure 6: Scoring Program execution flow

## 7 Conclusions and Outlook

We have prepared a dataset, challenge, and platform for developing and comparing machine learning methods that quantify uncertainties in addition to providing point estimates. This project builds on previous work in the context of the Higgs boson discovery at the Large Hadron Collider. With the growing size of datasets in high energy physics, the sophistication of tools, and the precision requirements to explore new phenomena, uncertainty quantification will be an essential part of machine learning going forward.

Building a challenge of this kind has itself been a challenge. We needed to ensure that the problem was realistic enough, manageable to non-experts, and useful. These requirements were often in conflict, e.g. we wanted systematic uncertainties to be most important, but we also needed the dataset size to not be too large so that non-experts could analyse them. We also appreciate that there is no unique metric for trading off accuracy and precision and we look forward to further discussions on the choice we made throughout the challenge period and beyond<sup>4</sup>.

While focused on high energy physics and the Higgs boson, the features of the competition are much more general. We hope that the lessons learned here will be valuable across high energy physics and beyond.

## Acknowledgements

We are grateful to the US Department of Energy, Office of High Energy Physics, subprogram on Computational High Energy Physics, for sponsoring this research. Discussions seminal to this work were hosted at Institut Pascal at Université Paris-Saclay with the support of the program “Investissements d’avenir” ANR-11-IDEX-0003-01.

## References

- [1] C. Adam-Bourdarios, G. Cowan, C. Germain, I. Guyon, B. Kégl, and D. Rousseau, *The Higgs boson machine learning challenge*, in *Proceedings of the NIPS 2014 Workshop on High-energy Physics and Machine Learning*, G. Cowan, C. Germain, I. Guyon, B. Kégl, and D. Rousseau, eds. PMLR, Montreal, Canada, 13 Dec, 2015.  
<http://proceedings.mlr.press/v42/cowa14.html>.
- [2] K. Cranmer, J. Pavez, and G. Louppe, *Approximating Likelihood Ratios with Calibrated Discriminative Classifiers*, [arXiv:1506.02169 \[stat.AP\]](#).
- [3] P. Baldi, K. Cranmer, T. Faucett, P. Sadowski, and D. Whiteson, *Parameterized neural networks for high-energy physics*, *Eur. Phys. J. C* **76** (2016) 235, [arXiv:1601.07913 \[hep-ex\]](#).
- [4] J. Brehmer, F. Kling, I. Espejo, and K. Cranmer, *MadMiner: Machine learning-based inference for particle physics*, *Comput. Softw. Big Sci.* **4** (2020) 3, [arXiv:1907.10621 \[hep-ph\]](#).
- [5] J. Brehmer, G. Louppe, J. Pavez, and K. Cranmer, *Mining gold from implicit models to improve likelihood-free inference*, *Proc. Nat. Acad. Sci.* (2020) 201915980, [arXiv:1805.12244 \[stat.ML\]](#).
- [6] J. Brehmer, K. Cranmer, G. Louppe, and J. Pavez, *Constraining Effective Field Theories with Machine Learning*, [arXiv:1805.00013 \[hep-ph\]](#).
- [7] J. Brehmer, K. Cranmer, G. Louppe, and J. Pavez, *A Guide to Constraining Effective Field Theories with Machine Learning*, [arXiv:1805.00020 \[hep-ph\]](#).
- [8] B. Nachman, *A guide for deploying Deep Learning in LHC searches: How to achieve optimality and account for uncertainty*, [arXiv:1909.03081 \[hep-ph\]](#).
- [9] A. Ghosh, B. Nachman, and D. Whiteson, *Uncertainty-aware machine learning for high energy physics*, *Phys. Rev. D* **104** (2021) 056026, [arXiv:2105.08742 \[physics.data-an\]](#).

---

<sup>4</sup>The dataset will continue to be available after the challenge and we hope that it will continue to provide a benchmark for method developments in the future.

- [10] A. Blance, M. Spannowsky, and P. Waite, *Adversarially-trained autoencoders for robust unsupervised new physics searches*, **JHEP** **10** (2019) 047, [arXiv:1905.10384 \[hep-ph\]](#).
- [11] C. Englert, P. Galler, P. Harris, and M. Spannowsky, *Machine Learning Uncertainties with Adversarial Neural Networks*, **Eur. Phys. J. C** **79** (2019) 4, [arXiv:1807.08763 \[hep-ph\]](#).
- [12] G. Louppe, M. Kagan, and K. Cranmer, *Learning to Pivot with Adversarial Networks*, [arXiv:1611.01046 \[stat.ME\]](#).
- [13] J. Dolen, P. Harris, S. Marzani, S. Rappoccio, and N. Tran, *Thinking outside the ROCs: Designing Decorrelated Taggers (DDT) for jet substructure*, **JHEP** **05** (2016) 156, [arXiv:1603.00027 \[hep-ph\]](#).
- [14] I. Mout, B. Nachman, and D. Neill, *Convolved Substructure: Analytically Decorrelating Jet Substructure Observables*, **JHEP** **05** (2018) 002, [arXiv:1710.06859 \[hep-ph\]](#).
- [15] J. Stevens and M. Williams, *uBoost: A boosting method for producing uniform selection efficiencies from multivariate classifiers*, **JINST** **8** (2013) P12013, [arXiv:1305.7248 \[nucl-ex\]](#).
- [16] C. Shimmin, P. Sadowski, P. Baldi, E. Weik, D. Whiteson, E. Goul, and A. Sogaard, *Decorrelated Jet Substructure Tagging using Adversarial Neural Networks*, [arXiv:1703.03507 \[hep-ex\]](#).
- [17] L. Bradshaw, R. K. Mishra, A. Mitridate, and B. Ostdiek, *Mass Agnostic Jet Taggers*, [arXiv:1908.08959 \[hep-ph\]](#).
- [18] ATLAS, T. A. Collaboration, *Performance of mass-decorrelated jet substructure observables for hadronic two-body decay tagging in ATLAS*, ATL-PHYS-PUB-2018-014 (2018) . <http://cds.cern.ch/record/2630973>.
- [19] G. Kasieczka and D. Shih, *DisCo Fever: Robust Networks Through Distance Correlation*, [arXiv:2001.05310 \[hep-ph\]](#).
- [20] S. Wunsch, S. Jörger, R. Wolf, and G. Quast, *Reducing the dependence of the neural network function to systematic uncertainties in the input space*, **Comput. Softw. Big Sci.** **4** (2020) 5, [arXiv:1907.11674 \[physics.data-an\]](#).
- [21] A. Rogozhnikov, A. Bukva, V. V. Gligorov, A. Ustyuzhanin, and M. Williams, *New approaches for boosting to uniformity*, **JINST** **10** (2015) T03002, [arXiv:1410.4140 \[hep-ex\]](#).
- [22] C. Collaboration, *A deep neural network to search for new long-lived particles decaying to jets*, **Machine Learning: Science and Technology** (2020) , 1912.12238.
- [23] J. M. Clavijo, P. Glaysheer, and J. M. Katzy, *Adversarial domain adaptation to reduce sample bias of a high energy physics classifier*, [arXiv:2005.00568 \[stat.ML\]](#).
- [24] G. Kasieczka, B. Nachman, M. D. Schwartz, and D. Shih, *ABCDiCo: Automating the ABCD Method with Machine Learning*, [arXiv:2007.14400 \[hep-ph\]](#).
- [25] O. Kitouni, B. Nachman, C. Weisser, and M. Williams, *Enhancing searches for resonances with machine learning and moment decomposition*, [arXiv:2010.09745 \[hep-ph\]](#).
- [26] V. Estrade, C. Germain, I. Guyon, and D. Rousseau, *Systematic aware learning - A case study in High Energy Physics*, **EPJ Web Conf.** **214** (2019) 06024.
- [27] A. Ghosh and B. Nachman, *A cautionary tale of decorrelating theory uncertainties*, **Eur. Phys. J. C** **82** (2022) 46, [arXiv:2109.08159 \[hep-ph\]](#).
- [28] S. Wunsch, S. Jörger, R. Wolf, and G. Quast, *Optimal statistical inference in the presence of systematic uncertainties using neural network optimization based on binned Poisson likelihoods with nuisance parameters*, **Comput. Softw. Big Sci.** **5** (2021) 4, [arXiv:2003.07186 \[physics.data-an\]](#).

- [29] A. Elwood, D. Krücker, and M. Shchedrolosiev, *Direct optimization of the discovery significance in machine learning for new physics searches in particle colliders*, *J. Phys. Conf. Ser.* **1525** (2020) 012110.
- [30] L.-G. Xia, *QBDT, a new boosting decision tree method with systematical uncertainties into training for High Energy Physics*, *Nucl. Instrum. Meth.* **A930** (2019) 15, [arXiv:1810.08387 \[physics.data-an\]](#).
- [31] P. De Castro and T. Dorigo, *INFERNO: Inference-Aware Neural Optimisation*, *Comput. Phys. Commun.* **244** (2019) 170, [arXiv:1806.04743 \[stat.ML\]](#).
- [32] T. Charnock, G. Lavaux, and B. D. Wandelt, *Automatic physical inference with information maximizing neural networks*, *Physical Review D* **97** (Apr, 2018) . <http://dx.doi.org/10.1103/PhysRevD.97.083004>.
- [33] J. Alsing and B. Wandelt, *Nuisance hardened data compression for fast likelihood-free inference*, *Mon. Not. Roy. Astron. Soc.* **488** (2019) 5093, [arXiv:1903.01473 \[astro-ph.CO\]](#).
- [34] N. Simpson and L. Heinrich, *neos: End-to-End-Optimised Summary Statistics for High Energy Physics*, *J. Phys. Conf. Ser.* **2438** (2023) 012105, [arXiv:2203.05570 \[physics.data-an\]](#).
- [35] P. Feichtinger et al., *Punzi-loss: a non-differentiable metric approximation for sensitivity optimisation in the search for new particles*, *Eur. Phys. J. C* **82** (2022) 121, [arXiv:2110.00810 \[hep-ex\]](#).
- [36] L. Layer, T. Dorigo, and G. Strong, *Application of Inferno to a Top Pair Cross Section Measurement with CMS Open Data*, [arXiv:2301.10358 \[hep-ex\]](#).
- [37] G. Kasieczka, M. Luchmann, F. Otterpohl, and T. Plehn, *Per-Object Systematics using Deep-Learned Calibration*, [arXiv:2003.11099 \[hep-ph\]](#).
- [38] S. Bollweg, M. Haußmann, G. Kasieczka, M. Luchmann, T. Plehn, and J. Thompson, *Deep-Learning Jets with Uncertainties and More*, *SciPost Phys.* **8** (2020) 006, [arXiv:1904.10004 \[hep-ph\]](#).
- [39] J. Y. Araz and M. Spannowsky, *Combine and Conquer: Event Reconstruction with Bayesian Ensemble Neural Networks*, *JHEP* **04** (2021) 296, [arXiv:2102.01078 \[hep-ph\]](#).
- [40] M. Bellagente, M. Haußmann, M. Luchmann, and T. Plehn, *Understanding Event-Generation Networks via Uncertainties*, [arXiv:2104.04543 \[hep-ph\]](#).
- [41] T. Y. Chen, B. Dey, A. Ghosh, M. Kagan, B. Nord, and N. Ramachandra, *Interpretable Uncertainty Quantification in AI for HEP*, in *Snowmass 2021*. 8, 2022. [arXiv:2208.03284 \[hep-ex\]](#).
- [42] S. Amrouche, L. Basara, P. Calafiura, V. Estrade, S. Farrell, D. R. Ferreira, L. Finnie, N. Finnie, C. Germain, V. V. Gligorov, T. Golling, S. Gorbunov, H. Gray, I. Guyon, M. Hushchyn, V. Innocente, M. Kiehn, E. Moyse, J.-F. Puget, Y. Reina, D. Rousseau, A. Salzburger, A. Ustyuzhanin, J.-R. Vlimant, J. S. Wind, T. Xylouris, and Y. Yilmaz, *The tracking machine learning challenge: Accuracy phase*, in *The NeurIPS 2018 Competition*, pp. 231–264. Springer International Publishing, Nov., 2019. [arXiv:1904.06778 \[hep-ex\]](#).
- [43] S. Amrouche, L. Basara, P. Calafiura, D. Emelianov, V. Estrade, S. Farrell, C. Germain, V. V. Gligorov, T. Golling, S. Gorbunov, H. Gray, I. Guyon, M. Hushchyn, V. Innocente, M. Kiehn, M. Kunze, E. Moyse, D. Rousseau, A. Salzburger, A. Ustyuzhanin, and J.-R. Vlimant, *The Tracking Machine Learning Challenge: Throughput Phase*, *Comput. Softw. Big Sci.* **7** (2023) 1, [arXiv:2105.01160 \[cs.LG\]](#).
- [44] G. Kasieczka, B. Nachman, D. Shih, O. Amram, A. Andreassen, K. Benkendorfer, B. Bortolato, G. Brooijmans, F. Canelli, J. H. Collins, B. Dai, F. F. De Freitas, B. M. Dillon, I.-M. Dinu, Z. Dong, J. Donini, J. Duarte, D. A. Faroughy, J. Gonski, P. Harris, A. Kahn, J. F. Kamenik, C. K. Khosa, P. Komiske, L. Le Pottier, P. Martín-Ramiro, A. Matevc, E. Metodieiev, V. Mikuni, C. W. Murphy, I. Ochoa, S. E. Park, M. Pierini, D. Rankin, V. Sanz, N. Sarda, U. Seljak,

- A. Smolkovic, G. Stein, C. M. Suarez, M. Szewc, J. Thaler, S. Tsan, S.-M. Udrescu, L. Vaslin, J.-R. Vlimant, D. Williams, and M. Yunus, *The lhc olympics 2020 a community challenge for anomaly detection in high energy physics*, *Reports on Progress in Physics* **84** (Dec., 2021) 124201. <http://dx.doi.org/10.1088/1361-6633/ac36b9>.
- [45] I. Guyon, L. Sun-Hosoya, M. Boullé, H. J. Escalante, S. Escalera, Z. Liu, D. Jajetic, B. Ray, M. Saeed, M. Sebag, A. Statnikov, W.-W. Tu, and E. Viegas, *Analysis of the AutoML Challenge Series 2015–2018*, pp. 177–219. Springer International Publishing, Cham, 2019. [https://doi.org/10.1007/978-3-030-05318-5\\_10](https://doi.org/10.1007/978-3-030-05318-5_10).
- [46] Z. Liu, A. Pavao, Z. Xu, S. Escalera, F. Ferreira, I. Guyon, S. Hong, F. Hutter, R. Ji, J. C. S. J. Junior, G. Li, M. Lindauer, Z. Luo, M. Madadi, T. Nierhoff, K. Niu, C. Pan, D. Stoll, S. Treguer, J. Wang, P. Wang, C. Wu, Y. Xiong, A. Zela, and Y. Zhang, *Winning solutions and post-challenge analyses of the ChaLearn AutoDL challenge 2019*, *IEEE Transactions on Pattern Analysis and Machine Intelligence* (2020) 17.
- [47] A. E. Baz, I. Ullah, and etal, *Lessons learned from the neurips 2021 metadl challenge: Backbone fine-tuning without episodic meta-learning dominates for few-shot learning image classification*, PMLR (2022, to appear) .
- [48] D. Carrión-Ojeda, H. Chen, A. E. Baz, S. Escalera, C. Guan, I. Guyon, I. Ullah, X. Wang, and W. Zhu, *Neurips’22 cross-domain metadl competition: Design and baseline results*, [arXiv:2208.14686 \[cs.LG\]](https://arxiv.org/abs/2208.14686).
- [49] I. Guyon, G. Dror, V. Lemaire, D. L. Silver, G. Taylor, and D. W. Aha, *Analysis of the ijcnv 2011 utl challenge*, *Neural Networks* **32** (2012) 174.
- [50] M. L. Danula Hettiachchi, *Crowd bias challenge*, 2021. <https://kaggle.com/competitions/crowd-bias-challenge>.
- [51] S. P. Federica Proietto, Giovanni Bellitto, *Ccai@unict 2023*, 2023. <https://kaggle.com/competitions/ccaiunict-2023>.
- [52] ATLAS Collaboration, *The atlas experiment at the cern large hadron collider*, *JINST* **3** (2008) S08003.
- [53] L. Evans and P. Bryant, *LHC machine*, *JINST* **3** (aug, 2008) S08001.
- [54] T. Sjöstrand, S. Ask, J. R. Christiansen, R. Corke, N. Desai, P. Ilten, S. Mrenna, S. Prestel, C. O. Rasmussen, and P. Z. Skands, *An introduction to PYTHIA 8.2*, *Comput. Phys. Commun.* **191** (2015) 159, [arXiv:1410.3012 \[hep-ph\]](https://arxiv.org/abs/1410.3012).
- [55] DELPHES 3, J. de Favereau, C. Delaere, P. Demin, A. Giammanco, V. Lemaître, A. Mertens, and M. Selvaggi, *DELPHES 3, A modular framework for fast simulation of a generic collider experiment*, *JHEP* **02** (2014) 057, [arXiv:1307.6346 \[hep-ex\]](https://arxiv.org/abs/1307.6346).
- [56] B. Nachman and T. Rudelius, *Evidence for conservatism in LHC SUSY searches*, *Eur. Phys. J. Plus* **127** (2012) 157, [arXiv:1209.3522 \[stat.AP\]](https://arxiv.org/abs/1209.3522).
- [57] B. Nachman and T. Rudelius, *A Meta-analysis of the 8 TeV ATLAS and CMS SUSY Searches*, *JHEP* **02** (2015) 004, [arXiv:1410.2270 \[hep-ph\]](https://arxiv.org/abs/1410.2270).
- [58] A. Paszke, S. Gross, F. Massa, A. Lerer, J. Bradbury, G. Chanan, T. Killeen, Z. Lin, N. Gimeshein, L. Antiga, A. Desmaison, A. Köpf, E. Yang, Z. DeVito, M. Raison, A. Tejani, S. Chilamkurthy, B. Steiner, L. Fang, J. Bai, and S. Chintala, *Pytorch: An imperative style, high-performance deep learning library*, [arXiv:1912.01703 \[cs.LG\]](https://arxiv.org/abs/1912.01703).
- [59] M. Abadi, A. Agarwal, P. Barham, E. Brevdo, Z. Chen, C. Citro, G. S. Corrado, A. Davis, J. Dean, M. Devin, S. Ghemawat, I. Goodfellow, A. Harp, G. Irving, M. Isard, Y. Jia, R. Jozefowicz, L. Kaiser, M. Kudlur, J. Levenberg, D. Mané, R. Monga, S. Moore, D. Murray, C. Olah, M. Schuster, J. Shlens, B. Steiner, I. Sutskever, K. Talwar, P. Tucker, V. Vanhoucke, V. Vasudevan, F. Viégas, O. Vinyals, P. Warden, M. Wattenberg, M. Wicke, Y. Yu, and X. Zheng, *TensorFlow: Large-scale machine learning on heterogeneous systems*, . <https://www.tensorflow.org/>. Software available from tensorflow.org.



- [60] F. Pedregosa, G. Varoquaux, A. Gramfort, V. Michel, B. Thirion, O. Grisel, M. Blondel, P. Prettenhofer, R. Weiss, V. Dubourg, J. Vanderplas, A. Passos, D. Cournapeau, M. Brucher, M. Perrot, and E. Duchesnay, *Scikit-learn: Machine learning in Python*, Journal of Machine Learning Research **12** (2011) 2825.
- [61] C. Adam-Bourdarios, G. Cowan, C. Germain, I. Guyon, B. Kegl, and D. Rousseau, *Learning to discover: the higgs boson machine learning challenge - documentation*, .  
<http://opendata.cern.ch/record/329>.
- [62] ATLAS, G. Aad et al., *Evidence for the Higgs-boson Yukawa coupling to tau leptons with the ATLAS detector*, *JHEP* **04** (2015) 117, [arXiv:1501.04943 \[hep-ex\]](https://arxiv.org/abs/1501.04943).
- [63] P. Baldi, P. Sadowski, and D. Whiteson, *Searching for Exotic Particles in High-Energy Physics with Deep Learning*, *Nature Commun.* **5** (2014) 4308, [arXiv:1402.4735 \[hep-ph\]](https://arxiv.org/abs/1402.4735).
- [64] P. Baldi, P. Sadowski, and D. Whiteson, *Enhanced higgs boson to tau+ tau- search with deep learning*, *Physical Review Letters* **114** (Mar., 2015) .  
<http://dx.doi.org/10.1103/PhysRevLett.114.111801>.



## A Proton collisions and detection

This appendix gives a very minimal introduction to what the Challenge data is about (primarily taken from [61]).

The LHC collides bunches of protons every 25 nanoseconds within each of its four experiments. Two colliding protons produce a small firework in which part of the kinetic energy of the protons is converted into new particles. Most resulting particles are very unstable and decay quickly into a cascade of lighter particles. The ATLAS detector measures properties of these surviving particles (the so-called final state): the type of the particle (electron, photon, muon, etc.), its energy, and the 3D direction of the particle. Based on these properties, the decayed parent particle's properties can be inferred, and the inference chain continues until the heaviest primary particles are reached.

The different types of particles or pseudo particles of interest for the challenge are electrons, muons, hadronic tau, jets, and missing transverse energy. Electrons, muons, and taus are the three leptons<sup>5</sup> from the standard model.

For this competition, we selected only events with exactly one electron or exactly one muon, and with exactly one hadronic tau. These two particles should be of opposite electric charge. Figure 1 shows the particles in the selected final state, whose parameters are provided in the data.

Electrons and muons live long enough to reach the detector, so their properties (energy and direction) can be measured directly. Conversely, Taus decay almost immediately after their creation into either an electron and two neutrinos, a muon and two neutrinos, or a bunch of hadrons (charged particles) and a neutrino. The bunch of hadrons can be identified as a pseudo particle called the hadronic tau. Jets are pseudo particles rather than real particles; they originate from a high-energy quark or gluon and appear in the detector as a collimated energy deposit associated with charged tracks. The measured momenta (see Appendix B for a short introduction to special relativity) of all the particles of the event is the primary information provided for the challenge.

We are using the conventional 3D direct reference frame of ATLAS throughout the document (see Figure 7): the  $z$  axis points along the horizontal beam line, and the  $x$  and  $y$  axes are in the transverse plane with the  $y$  axis pointing towards the top of the detector.  $\theta$  is the polar angle and  $\phi$  is the azimuthal angle. Transverse quantities are quantities projected on the  $x - y$  plane, or, equivalently, quantities for which the  $z$  component is omitted. Instead of the polar angle  $\theta$ , we often use the *pseudorapidity*  $\eta = -\ln \tan(\theta/2)$ ;  $\eta = 0$  corresponds to a particle in the  $x - y$  plane ( $\theta = \pi/2$ ),  $\eta = +\infty$  corresponds to a particle traveling along the  $z$ -axis ( $\theta = 0$ ) direction and  $\eta = -\infty$  to the opposite direction ( $\theta = \pi$ ). Particles can be identified in the  $\eta$  range in  $[-2.5, 2.5]$ . For  $|\eta| \in [2.5, 5]$ , their momentum is still measured but they cannot be identified. Particles with  $|\eta|$  beyond 5 escape detection along the beam pipe.

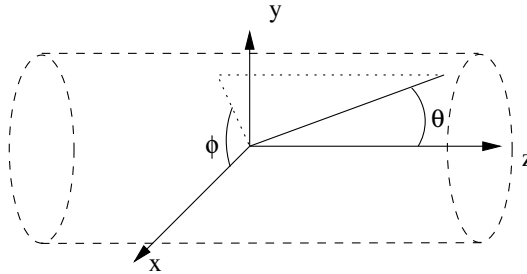


Figure 7: ATLAS reference frame

The missing transverse energy is a pseudo-particle which deserves a more detailed explanation. The neutrinos produced in the decay of a tau escape detection entirely. We can nevertheless infer their properties using the law of momentum conservation by computing the vectorial sum of the momenta of all the measured particles and subtracting it from the zero vector. In practice, measurement errors for all particles make the sum poorly estimated. Another difficulty is that many particles are lost

<sup>5</sup>For the list of elementary particles and their families, we refer the reader to <http://www.sciencemag.org/content/338/6114/1558.full>.

in the beam pipe along the  $z$  axis, so the information on momentum balance is lost in the direction of the  $z$  axis. Thus, we can carry out the summation only in the transverse plane, hence the name missing transverse energy, which is a 2D vector in the transverse plane.

To summarize, for each event, we produce a list of momenta for an electron or muon, a tau hadron, up to two jets, plus the missing transverse energy.

## B Special relativity

This appendix gives a very minimal introduction to special relativity for a better understanding of how the Higgs boson search is performed and what the extracted features mean (taken mainly from [61]).

### B.1 Momentum, mass, and energy

A fundamental equation of special relativity defines the so-called 4-momentum of a particle,

$$E^2 = p^2 c^2 + m^2 c^4, \quad (8)$$

where  $E$  is the energy of the particle,  $p$  is its momentum,  $m$  is the rest mass and  $c$  is the speed of light. When the particle is at rest, its momentum is zero, and so Einstein's well-known equivalence between mass and energy,  $E = mc^2$ , applies. In particle physics, we usually use the following units: GeV for energy, GeV/ $c$  for momentum, and GeV/ $c^2$  for mass. 1 GeV ( $10^9$  electron-Volt) is one billion times the energy acquired by an electron accelerated by a field of 1 V over 1 m, and it is also approximately the energy corresponding to the mass of a proton (more precisely, the mass of the proton is about 1 GeV/ $c^2$ ). When these units are used, Equation 8 simplifies to

$$E^2 = p^2 + m^2. \quad (9)$$

To avoid the clutter of writing GeV/ $c$  for momentum and GeV/ $c^2$  for mass, a shorthand of using GeV for all the three quantities of energy, momentum, and mass is usually adopted in most of the recent particle physics literature (including papers published by the ATLAS and the CMS experiments). We also adopt this convention throughout this document.

The momentum is related to the speed  $v$  of the particle. For a particle with non-zero mass, and when the speed of the particle is much smaller than the speed of light  $c$ , the momentum boils down to the classical formula  $p = mv$ . In special relativity, when the speed of the particle is comparable to  $c$ , we have  $p = \gamma mv$ , where

$$\gamma = \frac{1}{\sqrt{1 - (v/c)^2}}.$$

The relation holds both for the norms  $v$  and  $p$  and for the three dimensional vectors  $\vec{v}$  and  $\vec{p}$ , that is,  $\vec{p} = \gamma m \vec{v}$ , where, by convention,  $p = |\vec{p}|$  and  $v = |\vec{v}|$ . The factor  $\gamma$  diverges to infinity when  $v$  is close to  $c$ , and the speed of light cannot be reached nor surpassed. Hence, momentum is a concept more frequently used than speed in particle physics. The kinematics of a particle is fully defined by the momentum and energy, more precisely, by the 4-momentum  $(p_x, p_y, p_z, E)$ . When a particle is identified, it has a well-defined mass<sup>6</sup>, so its energy can be computed from the momentum and mass using Equation 8. Conversely, the mass of a particle with known momentum and energy can be obtained from

$$m = \sqrt{E^2 - p^2}. \quad (10)$$

Instead of specifying the momentum coordinate  $(p_x, p_y, p_z)$ , the parameters  $\phi$ ,  $\eta$ , and  $p_T = \sqrt{p_x^2 + p_y^2}$ , explained in Appendix A are often used.

### B.2 Invariant mass

The mass of a particle is an intrinsic property of a particle. So, for all events with a Higgs boson, the Higgs boson will have the same mass. To measure the mass of the Higgs boson, we need the 4-momentum  $(p_x, p_y, p_z, E) = (\vec{p}, E)$  of its decay products. Take the simple case of the Higgs boson  $H$  decaying into a final state of two particles,  $A$  and  $B$ , which are measured in the detector. By conservation of the energy and momentum (which are fundamental laws of nature), we can write  $E_H = E_A + E_B$  and  $\vec{p}_H = \vec{p}_A + \vec{p}_B$ . Since the energies and momenta of  $A$  and  $B$  are measured in the detector, we can compute  $E_H$  and  $p_H = |\vec{p}_H|$  and calculate  $m_H = \sqrt{E_H^2 - p_H^2}$ . This is called the invariant mass because (with a perfect detector)  $m_H$  remains the same even if  $E_H$  and  $p_H$  differ from event to event. This can be generalized to more than two particles in the final state and to any number of intermediate states.

---

<sup>6</sup>neglecting the particle width

In our case, the final state for particles originating from the Higgs boson is a lepton, a hadronic tau, and three neutrinos. The lepton and hadronic tau are measured in the detector, but for the neutrinos, all we have is the transverse missing energy, which estimates the sum of the momenta of the three neutrinos in the transverse plane. Hence, the mass of the  $\tau\tau$  can not be measured; we have to resort to different estimators which are only correlated to the mass of the  $\tau\tau$ . For example, the visible mass (feature DER\_mass\_vis) which is the invariant mass of the lepton and the hadronic tau, hence deliberately ignoring the unmeasured neutrinos. The possible jets in the events are not originating from the Higgs boson itself but can be produced in association with it.

### B.3 Other useful formulas

The following formulas are useful to compute DERived features from PRImary features (in [Appendix C](#)). For tau, lep, leading\_jet, and subleading\_jet, the momentum vector can be computed as

$$\vec{p} = \begin{pmatrix} p_x \\ p_y \\ p_z \end{pmatrix} = \begin{pmatrix} p_T \times \cos \phi \\ p_T \times \sin \phi \\ p_T \times \sinh \eta \end{pmatrix},$$

where  $p_T$  is the transverse momentum,  $\phi$  is the azimuth angle,  $\eta$  is the pseudo rapidity, and  $\sinh$  is the hyperbolic sine function. The modulus of  $p$  is

$$p_T \times \cosh \eta, \quad (11)$$

where  $\cosh$  is the hyperbolic cosine function. The mass of these particles is neglected, so  $E = p$ .

The missing transverse energy  $\vec{E}_T^{\text{miss}}$  is a two-dimensional vector

$$\vec{E}_T^{\text{miss}} = \begin{pmatrix} |\vec{E}_T^{\text{miss}}| \times \cos \phi_T \\ |\vec{E}_T^{\text{miss}}| \times \sin \phi_T \end{pmatrix},$$

where  $\phi_T$  is the azimuth angle of the missing transverse energy.

The invariant mass of two particles is the invariant mass of their 4-momentum sum, that is (still neglecting the mass of the two particles),

$$m_{\text{inv}}(\vec{a}, \vec{b}) = \sqrt{\left( \sqrt{a_x^2 + a_y^2 + a_z^2} + \sqrt{b_x^2 + b_y^2 + b_z^2} \right)^2 - (a_x + b_x)^2 - (a_y + b_y)^2 - (a_z + b_z)^2}. \quad (12)$$

The transverse mass of two particles is the invariant mass of the vector sum, but this time the third component is set to zero, which means only the projection on the transverse plane is considered. That is (still neglecting the mass of the two particles),

$$m_{\text{tr}}(\vec{a}, \vec{b}) = \sqrt{\left( \sqrt{a_x^2 + a_y^2} + \sqrt{b_x^2 + b_y^2} \right)^2 - (a_x + b_x)^2 - (a_y + b_y)^2}. \quad (13)$$

The pseudorapidity separation between two particles,  $A$  and  $B$ , is

$$|\eta_A - \eta_B|. \quad (14)$$

The  $R$  separation between two particles  $A$  and  $B$  is

$$\sqrt{(\eta_A - \eta_B)^2 + (\phi_A - \phi_B)^2}, \quad (15)$$

where  $\phi_A - \phi_B$  is brought back to the  $]-\pi, +\pi]$  range. A good intuition for the  $R$  separation is that it behaves like the 3D angle in radians between the two particles.

## C The detailed description of the features

In this section, we explain the list of features that describe the events.

Prefix-less variables `Weight`, `Label`, `DetailedLabel`, have a special role and should not be used as regular features for the model<sup>7</sup>:

`Weight` The event weight  $w_i$ . Not to be used as a feature. Not available in the test sample.

`Label` The event label (integer)  $y_i$  1 for signal, 0 for background . Not to be used as a feature. Not available in the test sample.

`DetailedLabel` The event detailed label (string) "htautau" for signal (when `Label==1`), "ztautau", "ttbar" and "diboson" for the three background categories (when `Label==0`). Not to be used as a feature. Not available in the test sample. This feature is used to implement some systematic biases; see [Appendix D](#). It could be used to train a multi-category classifier.

The variables prefixed with PRI (for PRIimitives) are “raw” quantities about the bunch collision as measured by the detector, essentially parameters of the momenta of particles.

In addition:

- Features are float unless specified otherwise.
- All azimuthal  $\phi$  angles are in radian in the  $]-\pi, +\pi]$  range.
- Energy, mass, and momentum are all in GeV
- All other features are unitless.
- Features are indicated as “undefined” when it can happen that they are meaningless or cannot be computed; in this case, their value is  $-25$ , which is outside the normal range of all variables.
- The mass of particles has not been provided, as it can safely be neglected for the challenge.

`PRI_had_pt` The transverse momentum  $\sqrt{p_x^2 + p_y^2}$  of the hadronic tau.

`PRI_had_eta` The pseudorapidity  $\eta$  of the hadronic tau.

`PRI_had_phi` The azimuth angle  $\phi$  of the hadronic tau.

`PRI_lep_pt` The transverse momentum  $\sqrt{p_x^2 + p_y^2}$  of the lepton (electron or muon).

`PRI_lep_eta` The pseudorapidity  $\eta$  of the lepton.

`PRI_lep_phi` The azimuth angle  $\phi$  of the lepton.

`PRI_met` The missing transverse energy  $\vec{E}_T^{\text{miss}}$ .

`PRI_met_phi` The azimuth angle  $\phi$  of the missing transverse energy vector.

`PRI_jet_num` The number of jets.

`PRI_jet_leading_pt` The transverse momentum  $\sqrt{p_x^2 + p_y^2}$  of the leading jet, that is the jet with the largest transverse momentum (undefined if `PRI_jet_num = 0`).

`PRI_jet_leading_eta` The pseudorapidity  $\eta$  of the leading jet (undefined if `PRI_jet_num = 0`).

`PRI_jet_leading_phi` The azimuth angle  $\phi$  of the leading jet (undefined if `PRI_jet_num = 0`).

`PRI_jet_subleading_pt` The transverse momentum  $\sqrt{p_x^2 + p_y^2}$  of the sub leading jet, that is, the jet with the second largest transverse momentum (undefined if `PRI_jet_num ≤ 1`).

`PRI_jet_subleading_eta` The pseudorapidity  $\eta$  of the subleading jet (undefined if `PRI_jet_num ≤ 1`).

`PRI_jet_subleading_phi` The azimuth angle  $\phi$  of the subleading jet (undefined if `PRI_jet_num ≤ 1`).

---

<sup>7</sup>In the starting kit they are split away in separated numpy arrays while the regular features are stored in a Dataframe

**PRI\_jet\_all\_pt** The scalar sum of the transverse momentum of all the jets of the events (not limited to the first 2).

Variables prefixed with DER (for DERived) are quantities computed from the primitive features on the fly from PRImary features (including possible systematics shifts)<sup>8</sup>. These quantities were selected by the physicists of ATLAS in the reference document [62] either to select regions of interest or as features for the Boosted Decision Trees used in this analysis in order to enhance signal Higgs boson events separation from background events. DERived features were already present in the HiggsML dataset [61]<sup>9</sup>. The DERived features correspond to feature engineering; an ideal model to be trained on infinite statistics should not need these features. This distinction between primary and derived features (or "low-level" and "high-level" or "raw variables" and "human-assisted variables") is rather standard in the AI for HEP literature, see for example [63, 64]. There is no guarantee that all DERived features are useful for this challenge (they could even be detrimental in the context of systematics). The challenge participant is free to keep these DERived features, remove them altogether, keep a few, or do more feature engineering.

**DER\_mass\_transverse\_met\_lep** The transverse mass (Equation 13) between the missing transverse energy and the lepton.

**DER\_mass\_vis** The invariant mass (Equation 12) of the hadronic tau and the lepton.

**DER\_pt\_h** The modulus (Equation 11) of the vector sum of the transverse momentum of the hadronic tau, the lepton, and the missing transverse energy vector.

**DER\_deltaeta\_jet\_jet** The absolute value of the pseudorapidity separation (Equation 14) between the two jets (undefined if  $\text{PRI\_jet\_num} \leq 1$ ).

**DER\_mass\_jet\_jet** The invariant mass (Equation 12) of the two jets (undefined if  $\text{PRI\_jet\_num} \leq 1$ ).

**DER\_prodelta\_jet\_jet** The product of the pseudorapidities of the two jets (undefined if  $\text{PRI\_jet\_num} \leq 1$ ).

**DER\_deltar\_had\_lep** The  $R$  separation (Equation 15) between the hadronic tau and the lepton.

**DER\_pt\_tot** The modulus (Equation 11) of the vector sum of the missing transverse momenta and the transverse momenta of the hadronic tau, the lepton, the leading jet (if  $\text{PRI\_jet\_num} \geq 1$ ) and the subleading jet (if  $\text{PRI\_jet\_num} = 2$ ) (but not of any additional jets).

**DER\_sum\_pt** The sum of the moduli (Equation 11) of the transverse momenta of the hadronic tau, the lepton, the leading jet (if  $\text{PRI\_jet\_num} \geq 1$ ) and the subleading jet (if  $\text{PRI\_jet\_num} = 2$ ) and the other jets (if  $\text{PRI\_jet\_num} \geq 3$ ).

**DER\_pt\_ratio\_lep\_tau** The ratio of the transverse momenta of the lepton and the hadronic tau.

**DER\_met\_phi\_centrality** The centrality of the azimuthal angle of the missing transverse energy vector w.r.t. the hadronic tau and the lepton

$$C = \frac{A + B}{\sqrt{A^2 + B^2}},$$

where  $A = \sin(\phi_{\text{met}} - \phi_{\text{lep}}) * \text{sign}(\sin(\phi_{\text{had}} - \phi_{\text{lep}}))$ ,  $B = \sin(\phi_{\text{had}} - \phi_{\text{met}}) * \text{sign}(\sin(\phi_{\text{had}} - \phi_{\text{lep}}))$ , and  $\phi_{\text{met}}$ ,  $\phi_{\text{lep}}$ , and  $\phi_{\text{had}}$  are the azimuthal angles of the missing transverse energy vector, the lepton, and the hadronic tau, respectively. The centrality is  $\sqrt{2}$  if the missing transverse energy vector  $\vec{E}_{\text{T}}^{\text{miss}}$  is on the bisector of the transverse momenta of the lepton and the hadronic tau. It decreases to 1 if  $\vec{E}_{\text{T}}^{\text{miss}}$  is collinear with one of these vectors and it decreases further to  $-\sqrt{2}$  when  $\vec{E}_{\text{T}}^{\text{miss}}$  is exactly opposite to the bisector. The logic behind this feature is that if the neutrinos are colinear to the lepton and the hadronic tau (which is a good approximation), then the missing transverse energy vector should be between the lepton and the hadronic tau.

<sup>8</sup>The code to compute DERived features from PRImitive features can be seen at [https://github.com/FAIR-Universe/HEP-Challenge/blob/master/ingestion\\_program/derived\\_quantities.py](https://github.com/FAIR-Universe/HEP-Challenge/blob/master/ingestion_program/derived_quantities.py)

<sup>9</sup>The notable exception of DER\_mass\_MMC which was in the HiggsML dataset but is deliberately absent from the Fair-Universe dataset because it was the result of a complex and lengthy Monte-Carlo Markov Chain integration which is not practical to rerun.

DER\_lep\_eta\_centrality The centrality of the pseudorapidity of the lepton w.r.t. the two jets (undefined if PRI\_jet\_num  $\leq 1$ )

$$\exp \left[ \frac{-4}{(\eta_1 - \eta_2)^2} \left( \eta_{\text{lep}} - \frac{\eta_1 + \eta_2}{2} \right)^2 \right],$$

where  $\eta_{\text{lep}}$  is the pseudorapidity of the lepton and  $\eta_1$  and  $\eta_2$  are the pseudorapidities of the two jets. The centrality is 1 when the lepton is on the bisector of the two jets, decreases to  $1/e$  when it is collinear to one of the jets, and decreases further to zero at infinity. The logic behind this feature is that if the two jets are emitted together with the Higgs boson, then the Higgs decay product should be in average between the two jets.

The feature list and event sample are primarily inspired from [62]. One crucial difference is that the dataset was produced with a more straightforward (leading-order) event generator (Pythia), and the detector effect was simulated with a more straightforward detector simulation (Delphes rather than Geant4 ATLAS Simulation). These simplifications allowed us to provide to participants a large sample allowing the development of sophisticated models while preserving the complexity of the original problem.

Variable	Mean	Sigma	Range
$\alpha_{\text{tes}}$	1.	0.01	[0.9, 1.1]
$\alpha_{\text{jes}}$	1.	0.01	[0.9, 1.1]
$\alpha_{\text{soft\_met}}$	0.	1.	[0., 5.]
$\alpha_{\text{ttbar\_scale}}$	1.	0.02	[0.8, 1.2]
$\alpha_{\text{diboson\_scale}}$	1.	0.25	[0., 2.]
$\alpha_{\text{bkg\_scale}}$	1.	0.001	[0.99, +1.01]

Table 2: List of six systematic bias Nuisance Parameter defined in the challenge, with the mean and sigma of their Gaussian (Log-normal for  $\alpha_{\text{soft\_met}}$ ) distribution and their range. The corresponding  $\alpha$  is set to the Mean value whenever a systematic bias is switched off. "No systematics" means all  $\alpha$  are set to their Mean value.

## D Systematic biases

This appendix details the implementation of the systematic biases Nuisance Parameters<sup>10</sup>.

### D.1 Systematic bias definition

Table 2 lists the different Nuisance Parameter with their Gaussian distribution and the range to which they are clipped.  $\alpha_{\text{tes}}$ ,  $\alpha_{\text{jes}}$ , and  $\alpha_{\text{soft\_met}}$  impacts some PRImary features, and then DERived features in cascade.  $\alpha_{\text{tes}}$  and  $\alpha_{\text{jes}}$  also impact which events make it to the final dataset.  $\alpha_{\text{ttbar\_scale}}$ ,  $\alpha_{\text{diboson\_scale}}$  and  $\alpha_{\text{bkg\_scale}}$  only impact the Weight of some background categories, that is to say, the composition of the background (for  $\alpha_{\text{ttbar\_scale}}$  and  $\alpha_{\text{diboson\_scale}}$ ) or the overall level of the background  $\alpha_{\text{bkg\_scale}}$ . The Gaussian distributions parameterise our ignorance of the exact value of the biases. We think their value is 1 (or zero for  $\alpha_{\text{soft\_met}}$ ) while their real value is slightly different, as parameterised by their width, thus biasing our measurement by an unknown amount, which can be simulated.

### D.2 Impact of biases on features

To detail the impact of the systematics, we need to detail first how the 4-momenta from the final state particles can be reconstructed from the PRImary features, following Appendix B. The four parameters ( $P_x, P_y, P_z, E$ ) of the four-vector of each particle in the final state can be reconstructed from the PRImary features as follows (using the hadronic tau as an example, and reminding that the mass is neglected so that  $E = P$ ),

$$P_{\text{had}} = \begin{pmatrix} \text{PRI\_had\_pt} * \cos(\text{PRI\_had\_phi}) \\ \text{PRI\_had\_pt} * \sin(\text{PRI\_had\_phi}) \\ \text{PRI\_had\_pt} * \sinh(\text{PRI\_had\_eta}) \\ \text{PRI\_had\_pt} * \cosh(\text{PRI\_had\_eta}) \end{pmatrix}$$

(where  $\sinh$  and  $\cosh$  are the hyperbolic sine and cosine functions), and similarly for  $P_{\text{lep}}$ ,  $P_{\text{leading jet}}$  and  $P_{\text{subleading jet}}$ .

The Missing ET vector is, by definition, in the transverse plane, so we have:

$$P_{\text{MET}} = \begin{pmatrix} \text{PRI\_met} * \cos(\text{PRI\_met\_phi}) \\ \text{PRI\_met} * \sin(\text{PRI\_met\_phi}) \\ \text{PRI\_met} \end{pmatrix}$$

$\alpha_{\text{tes}}$  is meant to describe the fact that the detector is not calibrated correctly for the measurement of the hadron momentum, meaning when the detector reports a momentum  $P_{\text{had}}$  it really is :

$$P_{\text{had}}^{\text{biased}} = \alpha_{\text{tes}} P_{\text{had}}$$

And similarly, for the jets momentum (when they are defined)

$$P_{\text{jet\_leading}}^{\text{biased}} = \alpha_{\text{jes}} P_{\text{jet\_leading}}$$

<sup>10</sup>See also [https://github.com/FAIR-Universe/HEP-Challenge/blob/master/ingestion\\_program/systematics.py](https://github.com/FAIR-Universe/HEP-Challenge/blob/master/ingestion_program/systematics.py)



$$P_{\text{jet\_subleading}}^{\text{biased}} = \alpha_{\text{jes}} P_{\text{jet\_subleading}}$$

$\alpha_{\text{tes}}$  and  $\alpha_{\text{jes}}$  also have an impact on  $P_{\text{MET}}$ :  $P_{\text{MET}}$  is obtained from the opposite of the sum of all visible objects in the event so that changing one of the visible objects (like  $P_{\text{had}}$ ,  $P_{\text{leading jet}}$  or  $P_{\text{subleading jet}}$ ) has a correlated impact on  $P_{\text{MET}}$  (this calculation is performed on the first two coordinates and  $E_{\text{MET}}$  is recalculated from their modulus):

$$P_{\text{MET}}^{\text{biased}} = P_{\text{MET}} + (1 - \alpha_{\text{tes}})P_{\text{had}} + (1 - \alpha_{\text{jes}})P_{\text{leading jet}} + (1 - \alpha_{\text{jes}})P_{\text{subleading jet}}$$

$\alpha_{\text{soft\_met}}$  has a different role; it expresses an additional noise source in the measurement of the missing ET vector, which is not present in the simulation. A random 2D vector of norm  $ET_{\text{soft}} = \text{Lognormal}(\alpha_{\text{soft\_met}})$  is added to  $P_{\text{MET}}$  (with different values event by event, by contrast with  $\alpha_{\text{soft\_met}}$ , which has a fixed value for a given pseudo-experiment) (this calculation is performed on the first two coordinates and  $E_{\text{MET}}$  is recalculated from their modulus):

$$P_{\text{MET}}^{\text{biased}} = P_{\text{MET}} + \begin{pmatrix} \text{Gauss}(0, ET_{\text{soft}}) \\ \text{Gauss}(0, ET_{\text{soft}}) \end{pmatrix}$$

The corresponding modified PRImary features are then recomputed to new biased values:  $\text{PRI\_had\_pt}$ ,  $\text{PRI\_leading\_jet\_pt}$ ,  $\text{PRI\_leading\_jet\_pt}$ ,  $\text{PRI\_met}$ , and  $\text{PRI\_met\_phi}$ .

In addition,

$$PRI\_jet\_all\_pt^{\text{biased}} = \alpha_{\text{jes}} \times PRI\_jet\_all\_pt$$

If the number of jets is three or more, the impact of  $\alpha_{\text{jes}}$  on missing ET cannot be calculated, given that detailed information on the additional jets (beyond two) is not available; this is a legitimate approximation as the total jet transverse momentum would be in most cases dominated by the first two leading.

DERived features are also impacted if they depend on these PRImary features (see [Appendix C](#)). Thus, for each of  $\alpha_{\text{tes}}$ ,  $\alpha_{\text{jes}}$  and  $\alpha_{\text{soft\_met}}$ , different features are impacted in a correlated way.

### D.3 Weight impacting bias implementation

$\alpha_{\text{bkg\_scale}}$ ,  $\alpha_{\text{ttbar\_scale}}$  and  $\alpha_{\text{diboson\_scale}}$  only impact the Weight of background events, more precisely:

- events with `DetailedLabel="ztautau"`:

$$\text{Weight}^{\text{bias}} = \alpha_{\text{bkg\_scale}} \times \text{Weight}$$

- events with `DetailedLabel="ttbar"`:

$$\text{Weight}^{\text{bias}} = \alpha_{\text{bkg\_scale}} \times \alpha_{\text{ttbar\_scale}} \times \text{Weight}$$

- events with `DetailedLabel="diboson"`:

$$\text{Weight}^{\text{bias}} = \alpha_{\text{bkg\_scale}} \times \alpha_{\text{diboson\_scale}} \times \text{Weight}$$

So  $\alpha_{\text{bkg\_scale}}$  only affects the overall level of the background but leaves the background distributions unchanged.  $\alpha_{\text{ttbar\_scale}}$  and  $\alpha_{\text{diboson\_scale}}$  impacts only the proportion of the smaller backgrounds (see [Table 1](#)), thus distorting the overall background distribution.

### D.4 Event selection

Hadronic tau (and also the jets) can only be identified in the detector above a certain transverse momentum threshold ("low threshold" in the following) so that the raw dataset  $\text{PRI\_had\_pt}$ ,  $\text{PRI\_jet\_leading\_pt}$ ,  $\text{PRI\_jet\_subleading\_pt}$  have clear thresholds. When applying  $\alpha_{\text{tes}}$  and  $\alpha_{\text{jes}}$ , these thresholds move so that if nothing else is done, the threshold position would be an obvious giveaway of the value of  $\alpha_{\text{tes}}$  and  $\alpha_{\text{jes}}$ .

To alleviate this, "high thresholds" (see [Table 3](#)) have been defined, which should systematically be applied after the calculation of the biased PRImary parameters, so that the thresholds to be observed on  $\text{PRI\_had\_pt}$ ,  $\text{PRI\_jet\_leading\_pt}$ ,  $\text{PRI\_jet\_subleading\_pt}$  are independent of  $\alpha_{\text{tes}}$  and  $\alpha_{\text{jes}}$ . The

Variable	Low threshold (GeV)	High threshold (GeV)
$P_{\text{had}}^T$	$\simeq 23$	26
$P_{\text{leading\_jet}}^T$ and $P_{\text{subleading\_jet}}^T$	$\simeq 23$	26

Table 3: Low and high threshold of hadronic tau and jet transverse momentum.

ranges in Table 2 are such that the thresholds should also be applied when no systematics bias is used<sup>11</sup>.

---

<sup>11</sup>In practice, function `systematics` in [https://github.com/FAIR-Universe/HEP-Challenge/blob/master/ingestion\\_program/systematics.py](https://github.com/FAIR-Universe/HEP-Challenge/blob/master/ingestion_program/systematics.py) should always be used, even in the no systematics case.